

Differential eNOS-signalling by platelet subpopulations regulates adhesion and aggregation

Aneta Radziwon-Balicka^{1†}, Gabriela Lesyk^{1†}, Valentina Back¹, Teresa Fong¹, Erica L. Loredon-Calderon¹, Bin Dong², Haitham El-Sikhry¹, Ahmed A. El-Sherbeni¹, Ayman El-Kadi¹, Stephen Ogg³, Arno Siraki¹, John M. Seubert^{1,4,5,6}, Maria Jose Santos-Martinez⁷, Marek W. Radomski⁸, Carlos A. Velazquez-Martinez¹, Ian R. Winship², and Paul Jurasz^{1,4,5,6*}

¹Faculty of Pharmacy and Pharmaceutical Sciences, University of Alberta, Edmonton, AB T6G-2E1, Canada; ²Neurochemical Research Unit, Department of Psychiatry, University of Alberta, Edmonton, AB T6G-2R3, Canada; ³Department of Medical Microbiology and Immunology, University of Alberta Edmonton, AB T6G-2E1, Canada; ⁴Department of Pharmacology, University of Alberta Edmonton, AB T6G-2H7, Canada; ⁵Cardiovascular Research Centre, University of Alberta, Edmonton, AB T6G-2S2, Canada; ⁶Mazankowski Heart Institute, Edmonton, AB T6G-2R7; ⁷School of Pharmacy and Pharmaceutical Sciences, Trinity College Dublin, Dublin, Ireland; and ⁸College of Medicine, University of Saskatchewan, Saskatoon, SK S7N-5E5, Canada

Received 7 June 2016; revised 1 December 2016; editorial decision 22 August 2017; accepted 1 September 2017; online publish-ahead-of-print 4 September 2017

Time for primary review: 60 days

Aims

In addition to maintaining haemostasis, circulating blood platelets are the cellular culprits that form occlusive thrombi in arteries and veins. Compared to blood leucocytes, which exist as functionally distinct subtypes, platelets are considered to be relatively simple cell fragments that form vascular system plugs without a differentially regulated cellular response. Hence, investigation into platelet subpopulations with distinct functional roles in haemostasis/thrombosis has been limited. In our present study, we investigated whether functionally distinct platelet subpopulations exist based on their ability to generate and respond to nitric oxide (NO), an endogenous platelet inhibitor.

Methods and results

Utilizing highly sensitive and selective flow cytometry protocols, we demonstrate that human platelet subpopulations exist based on the presence and absence of endothelial nitric oxide synthase (eNOS). Platelets lacking eNOS (approximately 20% of total platelets) fail to produce NO and have a down-regulated soluble guanylate cyclase-protein kinase G (sGC-PKG)-signalling pathway. In flow chamber and aggregation experiments eNOS-negative platelets primarily initiate adhesion to collagen, more readily activate integrin $\alpha_{IIb}\beta_3$ and secrete matrix metalloproteinase-2, and form larger aggregates than their eNOS-positive counterparts. Conversely, platelets having an intact eNOS-sGC-PKG-signalling pathway (approximately 80% of total platelets) form the bulk of an aggregate via increased thromboxane synthesis and ultimately limit its size via NO generation.

Conclusion

These findings reveal previously unrecognized characteristics and complexity of platelets and their regulation of adhesion/aggregation. The identification of platelet subpopulations also has potentially important consequences to human health and disease as impaired platelet NO-signalling has been identified in patients with coronary artery disease.

Keywords

Platelet subpopulations • Nitric oxide • Endothelial nitric oxide synthase • Aggregation • Flow cytometry

* Corresponding author. Tel: 780 492 2120, E-mail: jurasz@ualberta.ca

†The first two authors contributed equally to the study.

1. Introduction

Because platelets are anuclear they have long been considered simple and investigations into whether they exist as biochemically distinct subpopulations with differential functional roles in haemostasis and thrombosis have been limited.^{1–4} If not consumed in haemostatic/thrombotic reactions, within the human circulation platelets have a 7–10 day lifespan due to an internal apoptotic clock.⁵ When activated, such as by vascular injury or atherosclerotic plaque rupture, platelets undergo a series of reactions including adhesion to sub-endothelial proteins collagen and von Willebrand Factor (vWF) followed by platelet-platelet aggregation, which is primarily mediated by integrin $\alpha_{IIb}\beta_3$ (GPIIb/IIIa). In a growing platelet plug the aggregation process is repeated and amplified in a positive feedback cycle via platelet secretion of thromboxane A₂, ADP, matrix metalloproteinase-2 (MMP-2),⁶ as well as by other soluble mediators.

Several negative-feedback mechanisms inhibit aggregation, although these can be overwhelmed during thrombosis.⁷ The endothelium produces the anti-platelet aggregation factors prostacyclin and NO.^{8–11} Additionally, upon activation, platelets themselves generate NO^{12–14} inhibiting adhesion^{9,15} and aggregation.^{16,17} The biochemical pathway mediating NO's platelet inhibitory effects primarily involves sGC-PKG-signalling.¹⁸ PKG phosphorylates vasodilator-stimulated phosphoprotein (VASP) enabling VASP binding to the platelet cytoskeleton^{19,20} and inhibition of $\alpha_{IIb}\beta_3$ activation.^{21,22} PKG also suppresses $\alpha_{IIb}\beta_3$ activation via inositol-1, 4, 5-triphosphate receptor-associated cGMP kinase substrate-signalling²³ and inhibition of thromboxane receptor activation.²⁴ Platelet NOS activity has been attributed primarily to the eNOS (NOSIII) isoform,^{13,25} although the ability of platelets to produce NO has been questioned in recent years.²⁶ To explain some of these discrepancies in findings, we proposed that differences in platelet eNOS levels might account for a part of the divergent results. More importantly, we further hypothesized that if two platelet subpopulations exist based on differential NO-signalling, they may represent functionally distinct platelet subpopulations with differential roles in adhesion and aggregation.

2. Methods

Detailed materials and methods are available in the [Supplementary material online](#).

2.1 Platelet isolation

The study was approved by the University of Alberta Human Research Ethics Board and conforms to the Declaration of Helsinki. Following informed consent blood was obtained from healthy volunteers (22–40 years of age) who had not taken any drugs known to affect platelet function for 2 weeks prior to the study. Prostacyclin-washed platelet suspensions were prepared as described previously.²⁷

2.2 Detection of platelet NO production

DAF-FM fluorescence measurements were performed in washed platelets suspensions in Tyrode's buffer free of albumin. Briefly, human platelet-rich plasma was incubated with the fluorescent NO indicator DAF-FM diacetate (20 μ M) for 30 min at room temperature in the dark. Subsequently, DAF-FM-loaded platelets were pelleted, washed with Tyrode's buffer (3x) and resuspended at 2.5×10^8 /mL. Platelet DAF-FM fluorescence was measured by flow cytometry or fluorescence microscopy as described below and in the [Supplementary material online](#).

A Becton Dickinson FACScan flow cytometer with a 488 nm argon laser and 525 nm band-pass filter (FL1) was used to detect platelet DAF-FM fluorescence. Platelet DAF-FM fluorescence concentration was measured with a Beckman Coulter (Mississauga, ON, Canada) Quanta SC flow cytometer equipped with a 488 nm argon laser and 525 nm BP (FL1) and 568 nm BP filters (FL2) and a 620 nm LP filter. Measurements were carried out in FC (fluorescence concentration) mode, and 10 000 platelets stained with DAF-FM and anti-CD42b-PE antibody were analysed per experiment. Compensation was performed using Cell Lab Quanta analysis software to account for spectral overlap.

2.3 Flow cytometry

Flow cytometry for intracellular proteins was performed to investigate the eNOS-sGC-PKG pathway within platelets. Platelets were fixed in 4% formaldehyde in Tyrode's buffer (20 min) and then washed (3x) with PBS. Subsequently, platelets were permeabilized with 0.1% Triton X-100 in Tyrode's buffer and washed three times with PBS. The platelets were then resuspended in blocking buffer consisting of PBS + 5% BSA and incubated for 2 hrs at room temperature. To identify eNOS^{pos} and eNOS^{neg} subpopulations two-color intracellular flow cytometry was performed. Platelet samples were incubated with anti-eNOS clone M221 or concentration-matched isotype control IgG1 (1.25 μ g/mL) for 1 h at room temperature. In some control experiments the anti-eNOS clone 6H2 was utilized ([Supplementary material online, Figure S8B and C](#)). The samples were washed with PBS (3x) and incubated with DyLight 488-conjugated anti-mouse IgG (1:100) for 1 h in the dark. Finally, the platelets were washed with PBS and incubated with anti-CD42b-PE antibody (1:100) for 15 min and then diluted to a final volume of 1 mL with PBS before flow cytometry analysis.²¹ In addition, a control experiment was carried out to determine whether endothelial cell lysate neutralizes eNOS-antibody staining of platelets. Briefly, a T75 flask of human microvascular endothelial cells (HMVEC) was sonicated (2 x 5 s) in 1 mL of ice-cold PBS supplemented with 10% protease inhibitor cocktail (Sigma-Aldrich). Subsequently, the lysate was centrifuged at 10 000 g to separate out the lysate from the HMVEC membranes. Anti-eNOS antibody (1.25 μ g/mL) was then added to the HMVEC lysate or vehicle control and the staining protocol and subsequent flow cytometry carried out as described above.

To investigate the sGC-PKG-VASP pathway in eNOS^{pos} and eNOS^{neg} platelet subpopulations three-color flow cytometry was performed. Intracellular staining for platelet eNOS was carried out as described above. Subsequently, for sGC, PKG, or VASP determination, eNOS-stained platelets were then incubated with primary antibodies (anti-sGC 10 μ g/mL; anti-PKG1 10 μ g/mL; anti-VASP 2 μ g/mL) or corresponding concentration-matched isotype/IgG controls overnight at 4 °C. Next, the platelets were washed with PBS (3x). Following, samples were incubated in the dark with PE-conjugated or PerCP-conjugated secondary antibodies (1:100) for the detection of sGC, VASP, or PKG, respectively. Platelets were then washed with PBS and incubated with anti-CD42b-PE antibody (for PKG samples) or anti-CD41a-PE-Cy7 (for sGC and VASP samples) for 15 min and then diluted to a final volume of 1 mL with PBS before analysis by flow cytometry.

Flow cytometry was carried out with a Quanta SC flow cytometer. FSD (fluorescence surface density) and FC measurements were made and 10 000 platelet-specific events were analysed for each experiment. Unlike a traditional flow cytometer, which determines size based on forward light scatter (FS), the Quanta SC which we utilize uses the 'Coulter principle' (measures change in electrical resistance produced by cells suspended in electrolyte) to determine event volume. Quanta SC software

then calculates an event's fluorescence concentration or fluorescence surface density based on event volume. Compensation was performed using Cell Lab Quanta analysis software to account for spectral overlap.

2.4 Confocal microscopy

Confocal microscopy was performed to study eNOS expression by eNOS^{neg} and eNOS^{pos} platelets subpopulations. Platelets were fixed for 20 min in 4% formaldehyde in Tyrode's buffer, cytospinned onto 0.1% poly-lysine-coated coverslips, washed with PBS (3x) and permeabilized with Tyrode's buffer containing 0.1% Triton X-100 for 30 min. Specimens were blocked for 2 h in PBS with 5% BSA, followed by incubation with anti-eNOS (clone M221) or isotype control IgG1 antibodies (1:100 dilution) for 2 h. Coverslips were washed with PBS (3x), incubated with Alexa Fluor 488-conjugated goat (F(ab')₂) anti-mouse IgG for 1 h, and then washed three times with PBS. Subsequently, eNOS-stained coverslips were incubated with anti-CD42b-PE antibody (BD, Pharmingen) (1:100 dilution) or in some experiments Alexa Fluor 568 Phalloidin (Invitrogen) (1: 250) to detect F-actin. In other experiments coverslips were incubated with anti-caveolin-1 antibody (Abcam) (15 µg/mL) and then following washing with PerCP-conjugated anti-rabbit IgG (1:100) for 1 h. Coverslips were washed once again three times with PBS. Preparations were mounted in Prolong Gold Antifade solution (Invitrogen, Carlsbad, CA, USA) and analysed at room temperature on a Leica TCS SP5 microscope with a Leica inverted DMI 6000 B microscope base equipped with a 100x/1.4 oil NA objective. Electronic shutters and image acquisition were under the control of Leica LAF AS software. Fluorescence was excited with the 488 nm and in some experiments 543 nm laser lines. Finally, images were equally adjusted for contrast and brightness.

2.5 Statistics

Statistics were performed using Graph Pad Prism 7.0. All means are reported with SE. One-way ANOVA with Dunnet's multiple comparisons test and paired Student's *t*-tests (one- and two-sided) were performed where appropriate. Each N represents an experiment from an independent blood donor. A *P*-value less than 0.05 was considered significant.

3. Results

We established a NO-specific flow cytometry protocol using DAF-FM diacetate to measure human platelet NO production (Figure 1A–C). Using this protocol, we found that platelets generate a low level of NO even when non-activated and consistent with previous studies greatly increase NO-production upon aggregation (Figure 1A–C).^{12–14} Importantly, we identified a platelet subpopulation that basally does not produce NO, even in the presence of exogenous NOS substrate L-arginine, by specifically gating on a subpopulation of platelets tailing off the main NO-producing population in the bottom half of the FL1 first log decade (Figure 1D– gate R5). To account for differences in DAF-FM fluorescence due to potential differences in platelet volumes, we measured platelet DAF-FM fluorescence concentration. This revealed two distinct overlapping fluorescence peaks, and within isolates from healthy blood donors in the presence of L-arg NO-producing and non/low-level-producing platelets comprised 82.1 ± 2.4 and 17.9 ± 2.4% of total platelets, respectively (Figure 1E). Importantly, the NOS inhibitor L-NAME, but not superoxide dismutase (SOD) or the cell-permeable SOD mimetic TEMPOL, reduced the mean fluorescence of DAF-FM-

stained platelets (Figure 1F), confirming DAF-FM's specificity for NO. This specificity was further confirmed by vascular endothelial growth factor, a classical eNOS activating agonist, which increased the number of DAF-FM positive endothelial cells in culture (see Supplementary material online, Figure S1) and by the detection of the benzotriazole derivate (NO-bound form) of DAF-FM (see Supplementary material online, Figure S2). Finally, platelet NO production was further confirmed by a non-DAF-FM copper-based fluorescent NO probe CuFL2E (see Supplementary material online, Figure S3).

Because others have suggested that contaminating leucocytes account for platelet NO-production,²⁶ we established the purity of our isolations where on average less than 2 leucocytes/100 000 platelets were detected (see Supplementary material online, Figure S4). Based on leucocyte NO production (0.25–0.3 nmol/min/10⁶ cells),^{28,29} this low contamination level cannot account for the 0.4 µmol/L of NO reported previously to be produced by 10⁸ platelets when measured directly with a porphyrinic microsensor,¹⁴ or the 10⁶/mL leucocytes required to inhibit platelet aggregation.³⁰ Moreover, the presence of non/low-NO-producing and NO-producing platelets was confirmed using fluorescence microscopy (see Supplementary material online, Figure S5), and video fluorescence microscopy of DAF-FM-labeled platelets demonstrated that NO is generated by platelets upon adhesion and aggregation to collagen in the absence of leucocytes (see Supplementary material online, Videos 1 and 2). The platelet-generated NO serves as a negative-feedback mechanism limiting aggregation irrespective of whether a high or low concentration of agonists, such as collagen or thrombin stimulates platelets (Figure 2), although platelet-generated NO is more effective at inhibiting aggregation in response to low concentrations of agonists. This finding discounts the likelihood of a reported agonist concentration-dependent biphasic effect of NO on platelet aggregation.^{31,32} The NOS activity within NO-producing platelets mediating this negative feedback appears to be constitutive because 1400 W, an iNOS (NOSII)-selective inhibitor, failed to reverse the platelet inhibitory effects of L-arg (Figure 2B), as well as it failed to reduce the mean fluorescence of DAF-FM-stained activated platelets (see Supplementary material online, Figure S6). Importantly, similar to previous reports that identified platelet NOS as NOSIII (endothelial),^{12,25} an eNOS-selective inhibitory peptide AP-Cav-AB³³ enhanced platelet aggregation and reduced platelet DAF-FM fluorescence compared to control (see Supplementary material online, Figure S7A–C).

Thus, we used intracellular flow cytometry to investigate whether non-NO-producing and NO-producing platelets corresponded to platelets deficient and abundant in eNOS, respectively. Using this sensitive methodology we established that indeed two distinct platelet subpopulations exist, one lacking and one having eNOS (Figure 3A and B). Two-color flow cytometry for the platelet marker CD42b and eNOS confirmed that these are true platelet subpopulations and not contaminating endothelial cell or leucocyte microparticles (Figure 3A). Platelet eNOS fluorescence surface density (FSD) (Figure 3A, right histogram) was further measured as eNOS localizes to plasma membrane caveolae in endothelial cells,³⁴ and it co-localized with caveolin-1 in eNOS-immunoreactive platelets (see Supplementary material online, Figure S8A). The FSD measurements allowed us to account for platelet size and to exclude the possibility that low/absent eNOS fluorescence resulted from smaller platelets. Moreover, the presence of a bimodal FSD distribution (i.e. two peaks Figure 3A right histogram) demonstrates two distinct eNOS-based platelet subpopulations and not a continuum nor a Gaussian distribution of eNOS content. The eNOS-positive (eNOS^{pos}) and eNOS-negative (eNOS^{neg}) subpopulations in the blood of healthy adults accounted for

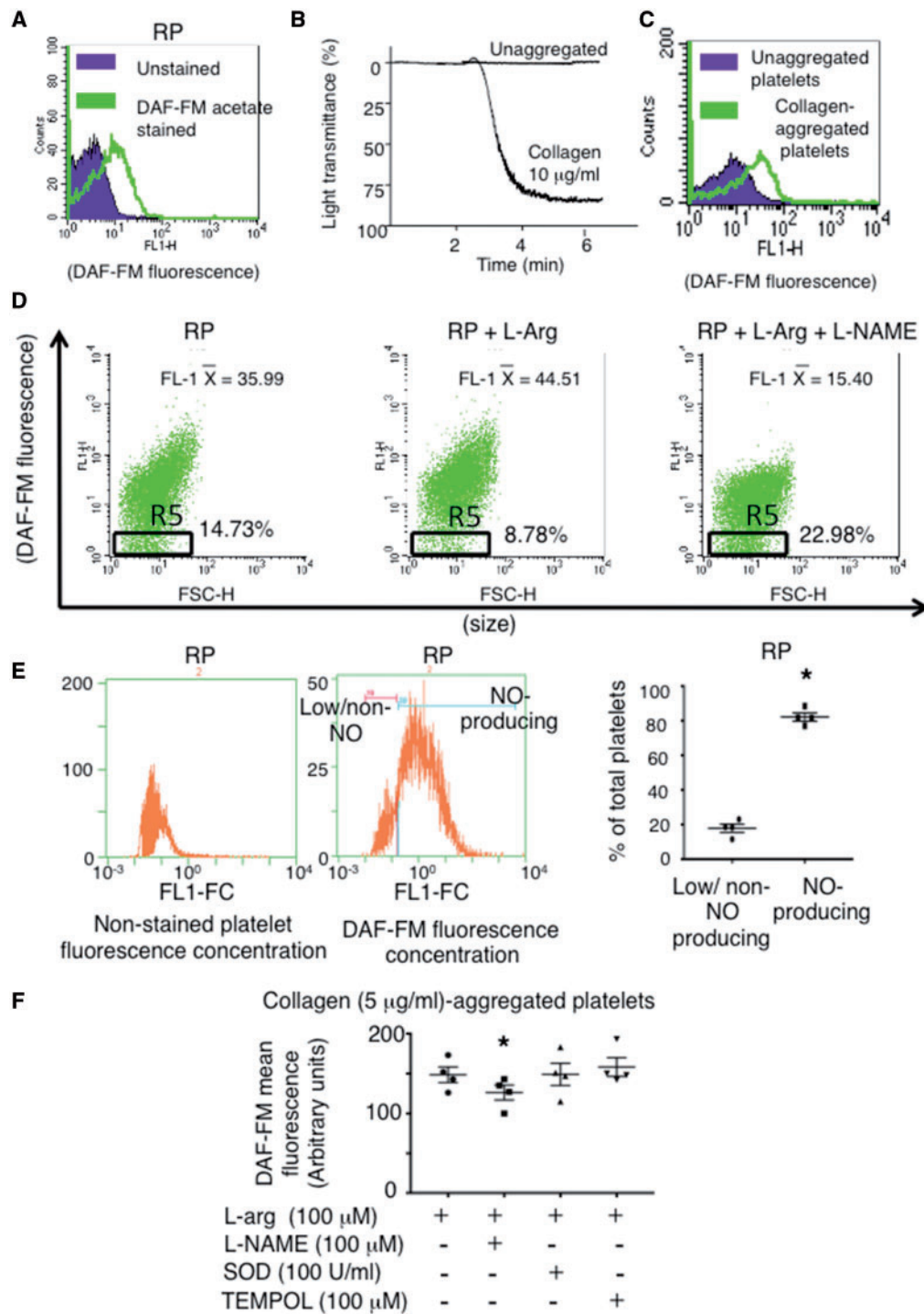


Figure 1 Identification of NO-producing and non/low-NO-producing Platelet Subpopulations. (A) Histogram overlay of unstained and DAF-FM-stained resting platelets (RP). (B) Platelet aggregometry traces and (C) histogram overlay of DAF-FM-stained unaggregated and collagen (10 µg/mL)-aggregated platelets. (D) Dot plots demonstrating a proportion of platelets remain low/non-NO-producers (Gate R5—middle panel) even when incubated with L-arg (30 µmol/L). FL-1 \bar{X} = mean fluorescence. (E) Representative non-stained and DAF-FM-stained platelet fluorescence concentration histograms and summary data quantifying the percentage of low/non-NO producing to NO-producing platelets. $N = 4$. * $P < 0.05$. (F) Summary data of platelet DAF-FM flow cytometry confirming the specificity of DAF-FM for NO. The NOS inhibitor L-NAME reduces DAF-FM fluorescence, while SOD and a cell permeable SOD mimetic (TEMPOL) do not. $N = 4$. ** $P < 0.01$ vs. L-arg. All representative dot plots and histograms are from at least $N = 3$ independent experiments.

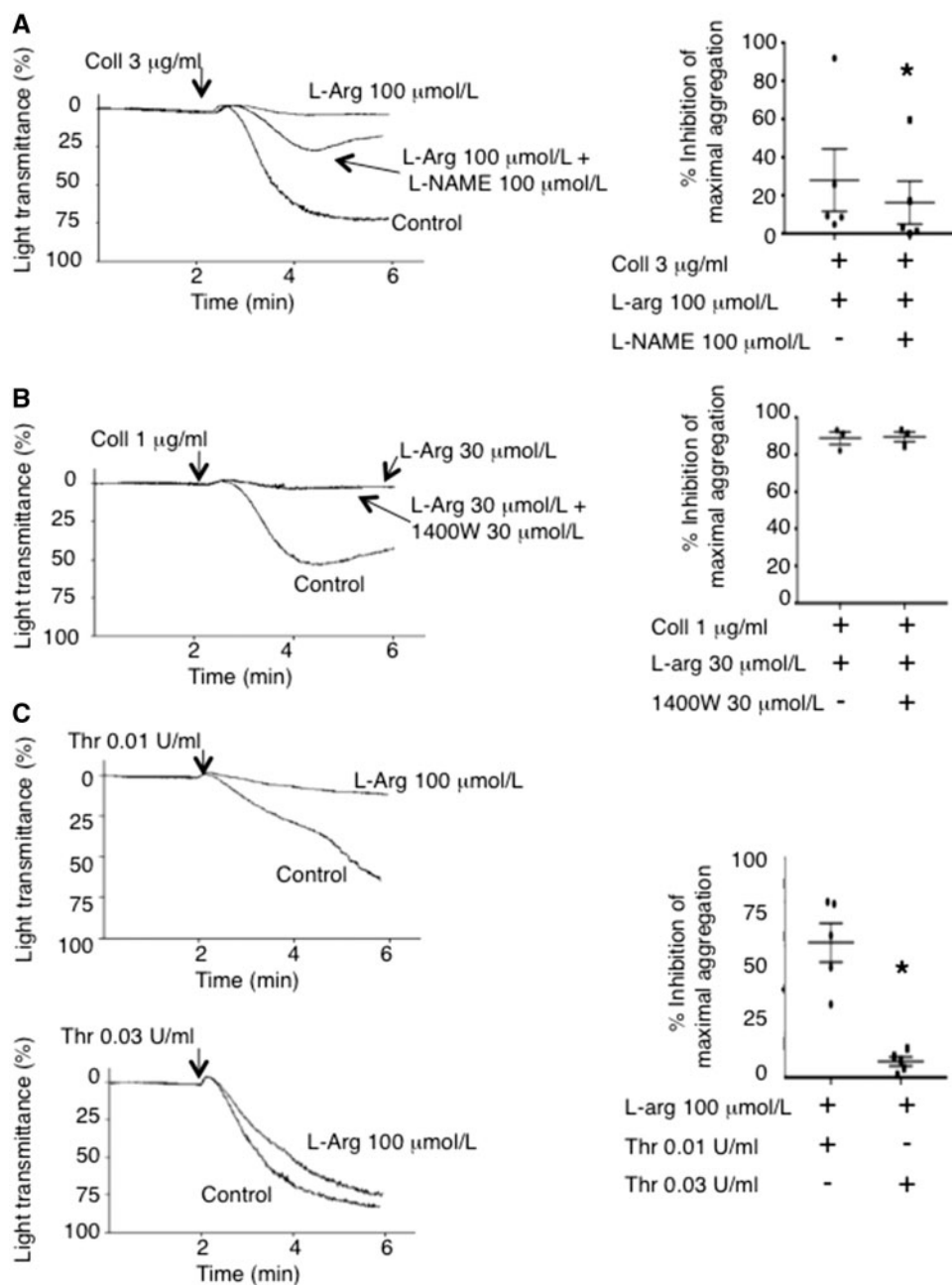


Figure 2 Platelet-derived NO Limits Aggregate Formation. (A) Representative traces and summary aggregation data of platelets stimulated by a high concentration of collagen (Coll 3 µg/mL) demonstrating that the NOS inhibitor L-NAME reverses the aggregation inhibitory effects of L-arginine. $N = 5$. *, $P < 0.05$. (B) Representative traces and summary aggregation data of platelets stimulated by a lower concentration of collagen (1 µg/mL) demonstrating that the selective iNOS inhibitor 1400 W fails to reverse the aggregation inhibitory effects of L-arginine. $N = 3$. $P > 0.05$. (C) Representative traces and summary aggregation data of platelets stimulated by low (0.01 U/mL) and high (0.03 U/mL) concentrations of thrombin demonstrating that platelet NO production inhibits aggregation at low thrombin concentrations. $N = 5$. *, $P < 0.05$.

80.6 ± 3.3 and 19.4 ± 3.2% of total platelets, respectively, corroborating the DAF-FM findings of NO-producing and non/low-NO-producing platelets (Figure 3B vs. Figure 1E). The existence of eNOS^{pos} and eNOS^{neg} subpopulations was confirmed via flow cytometry with a second eNOS N-terminal-specific antibody (see Supplementary material online, Figure S8B) and using immunofluorescence microscopy (Figure 3C). Importantly, compared to endothelial cells in which eNOS is highly abundant and

within the cytoplasm and membrane bound, platelet eNOS is of relative low abundance and membrane bound (Figure 3C–E). In line with these findings, eNOS mRNA in megakaryoblast cells (Meg-01) is similarly lower relative to endothelial cells (see Supplementary material online, Figure S9).

Fluorescence activated cell sorting (FACS) of DAF-FM-negative platelets resulted in an approximately 4-fold enrichment of eNOS^{neg} and a concomitant reduction in eNOS^{pos} platelets, confirming that non/low-NO-

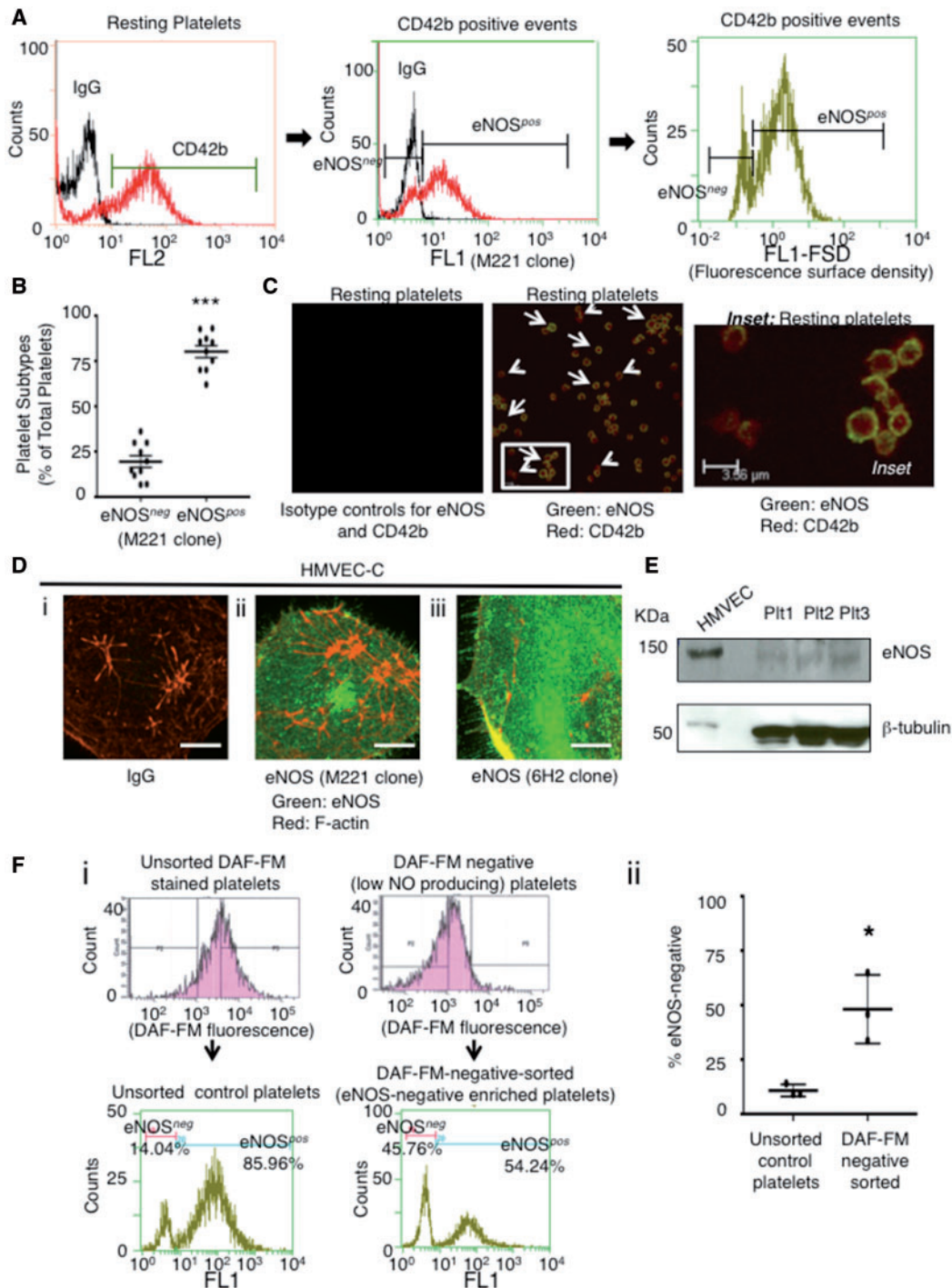


Figure 3 Identification of eNOS-based Platelet Subpopulations. (A) Histogram overlay of CD42b-positive events (*left histogram*) further sub-gated (*middle histogram*) demonstrating eNOS^{neg} and eNOS^{pos} platelets (isotype control IgG—black; eNOS—red) and platelet eNOS fluorescence surface density (*right histogram*). (B) Summary data comparing percentage of eNOS^{neg} to eNOS^{pos} platelets. $N = 10$. *** $P < 0.0001$. (C) Confocal microscopy of eNOS^{neg} (small arrows) and eNOS^{pos} (large arrows) platelets. (D) (i-iii) confocal microscopy of eNOS within cardiac-derived human microvascular endothelial cells (HMVEC-C). Scale bars = 20 μ m. All representative images from at least $N = 3$ independent experiments. (E) An immunoblot comparing eNOS in HMVEC and human platelets (Plt) from 3 donors. (F) (i) Representative platelet DAF-FM and eNOS^{neg}/eNOS^{pos} fluorescence histograms prior to and following FACS and (ii) summary data demonstrating that DAF-FM based sorting changes levels of eNOS^{neg} to eNOS^{pos} platelets. $N = 3$. * $P < 0.05$.

producing and NO-producing platelets are eNOS^{neg} and eNOS^{pos} platelets, respectively (Figure 3F). Moreover, the loading of DAF-FM diacetate into the platelet subpopulations is likely equal because they expressed equivalent acetyl esterase levels, an enzyme that converts DAF-FM diacetate to DAF-FM trapping the NO indicator within platelets (see Supplementary material online, Figure S10). The presence of eNOS within platelets and eNOS-based platelet subpopulations was also confirmed in eNOS-GFP transgenic mice³⁵ (see Supplementary material online, Figure S11). However, only 2.2 ± 0.7% of mouse platelets expressed eNOS suggesting marked differences in platelet NO-signalling exist between species.

To ensure that eNOS^{neg} platelets are not platelet microparticles that have lost eNOS or are near the end of their circulating lifespan, the volume and activated caspase-3 status of these subpopulations were compared. There was no significant difference in mean platelet volume between eNOS^{neg} vs. eNOS^{pos} platelets (6.3 ± 0.9 vs. 6.5 ± 1.0 μm³, respectively; *P* > 0.05) (see Supplementary material online, Figure S12). Importantly, their mean platelet volumes were nearly identical to those reported previously for platelets (6.5 μm³) indicating neither subpopulation were microparticles.² Because anuclear programmed cell death limits platelet lifespan,⁵ we developed a flow cytometry protocol to measure intra-platelet activated caspase-3 (see Supplementary material online, Figure S13A and B). Data demonstrating that eNOS^{neg} and eNOS^{pos} platelets displayed equivalent protein levels of activated caspase-3 (see Supplementary material online, Figure S13C and D) indicated that eNOS^{neg} platelets are of the same circulatory age as their eNOS^{pos} counterparts.

To determine whether biochemical differences exist between eNOS^{neg} and eNOS^{pos} platelets downstream of NO we investigated their sGC-PKG pathways. Following antibody characterization (see Supplementary material online, Figure S14A–F), flow cytometry for intra-platelet eNOS-pathway signalling proteins revealed that eNOS^{neg} platelets have lower protein levels of sGC, PKGI, and VASP than eNOS^{pos} platelets and FACS-sorted DAF-FM-negative platelets generate less cGMP upon activation than their DAF-FM-positive counterparts (Figure 4A–D). Because PKG phosphorylates VASP causing it to localize to integrin α_{IIb}β₃ focal adhesion sites and inhibit fibrinogen-binding,²² we investigated whether absent/down-regulated NOS-sGC-PKG-VASP signalling in eNOS^{neg} platelets resulted in enhanced α_{IIb}β₃ activation in this subpopulation. Upon stimulation by collagen, a significantly greater percentage of eNOS^{neg} platelets demonstrated activated integrin α_{IIb}β₃ than their eNOS^{pos} counterparts (Figure 4E).

Based on these biochemical differences between eNOS^{neg} and eNOS^{pos} platelets, we hypothesized that eNOS^{neg} platelets may be more likely to initiate adhesion and aggregation reactions as they have low/lack eNOS and have a down-regulated eNOS-signalling pathway, while eNOS^{pos} platelets limit aggregate formation via NO generation as the addition of L-arginine to platelets inhibits aggregation (Figure 2). To test this hypothesis, we first quantified the binding of eNOS-based platelet subpopulations to collagen under flow conditions in the presence of L-arginine. Flow cytometry of platelets that passed through a collagen-coated flow chamber (see Supplementary material online, Video 2) demonstrated a significant decrease in eNOS^{neg} platelets compared to pre-flow chamber controls (eNOS^{neg} pre-flow chamber 22.2 ± 3.4% vs. 18.1 ± 4.1% of total platelets post-flow chamber; *P* < 0.05), confirming their preferential initial adhesion (Figure 5A). In support of these quantitative experiments, we performed qualitative microscopy experiments on DAF-FM-stained platelets that were activated with collagen in the presence of L-arginine in the platelet aggregometer (Figure 5B). During early stages of aggregation, fluorescence microscopy of DAF-FM-stained platelets demonstrated that non-NO-producing platelets were bound primarily to free

strands of collagen as well to NO-producing platelets (Figure 5B i–iv). To further confirm preferential initial adhesion to collagen by non-NO-producing platelets video fluorescence microscopy of DAF-FM stained platelets was performed. The microscopy revealed that, at early time points (0–5 min), significantly more non-NO-producing platelets bound collagen than NO-producers (Figure 6A, Bi and see Supplementary material online, Video 1). The reverse was true at later time points (5–15 min) (Figure 6A, Bii and see Supplementary material online, Video 1). Subsequently, platelets were allowed to aggregate for a further 45 min and samples were taken for eNOS-immunofluorescence confocal microscopy following fixation, permeabilization and DAF-FM washout. Confocal microscopy-derived Z-stacks of these aggregates demonstrated low eNOS-immunofluorescence near the base with increasing eNOS: F-actin immunofluorescence from the bottom to the top of the aggregates (see Supplementary material online, Figure S15). To further test the hypothesis that eNOS^{pos} platelets limit aggregate formation via NO generation, we compared the aggregation responses of FACS-sorted DAF-FM-negative vs. -positive platelets (eNOS^{neg}- vs. eNOS^{pos}-enriched). As the viability of platelets *in vitro* is limited to a few hours, FACS sorting was unable to yield enough platelets in a timely manner to compare the two subpopulations by light-transmittance aggregometry. Nonetheless, in response to collagen FACS-sorted DAF-FM-negative platelets formed significantly larger aggregates as measured by area than their DAF-FM-positive counterparts indicating eNOS-positive platelets limit aggregate size (see Supplementary material online, Figure S16).

Finally, in an effort to address the questions of why a clot would not be entirely formed of eNOS^{neg} platelets and why eNOS^{pos} platelets may out compete their eNOS^{neg} counterparts during the aggregation phase, we investigated whether differences exist within platelet aggregation signalling components and whether any are enriched in one subpopulation compared to another. We focused on the MMP-2 pathway of aggregation⁶ as peak secretion of pro-MMP-2 occurs early on in the platelet aggregation process (Figure 7A), and the cyclooxygenase pathway as thromboxane has been demonstrated to play a dominant role in the secondary aggregation of platelets.³⁶ Once again, we developed flow cytometry protocols to measure intra-platelet MMP-2 and COX-1 (see Supplementary material online, Figures S17 and 18). Because in addition to being secreted, platelet MMP-2 translocates to the platelet membrane upon aggregation where it becomes active MMP-2,^{37,38} we also activated platelets under non-stirring conditions with collagen and measured platelet surface MMP-2 by flow cytometry. Fluorescence surface density measurements demonstrated higher levels of MMP-2 on eNOS^{neg} than eNOS^{pos} platelets (Figure 7B), and gelatin zymography revealed higher pro-MMP-2 levels in platelet lysates of FACS-sorted DAF-FM-negative than DAF-FM-positive platelets (Figure 7C). Conversely, flow cytometry fluorescence concentration measurements revealed eNOS^{pos} platelets have higher COX-1 protein levels than eNOS^{neg} platelets (Figure 7D). Consistent with these results FACS-sorted DAF-FM-positive platelets generated significantly more thromboxane than FACS-sorted DAF-FM-negative platelets as determined by the measurement of the stable metabolite TXB₂ (43 ± 9.2 vs. 25 ± 6.9 ng/10⁸ platelets; *P* < 0.05) (Figure 7E).

4. Discussion

4.1 Platelet-derived NO and eNOS-based subpopulations

Studies in the 1990's demonstrated that activated platelets generate NO, which inhibits aggregation, via a Ca²⁺-dependent NOS.^{12,13} In

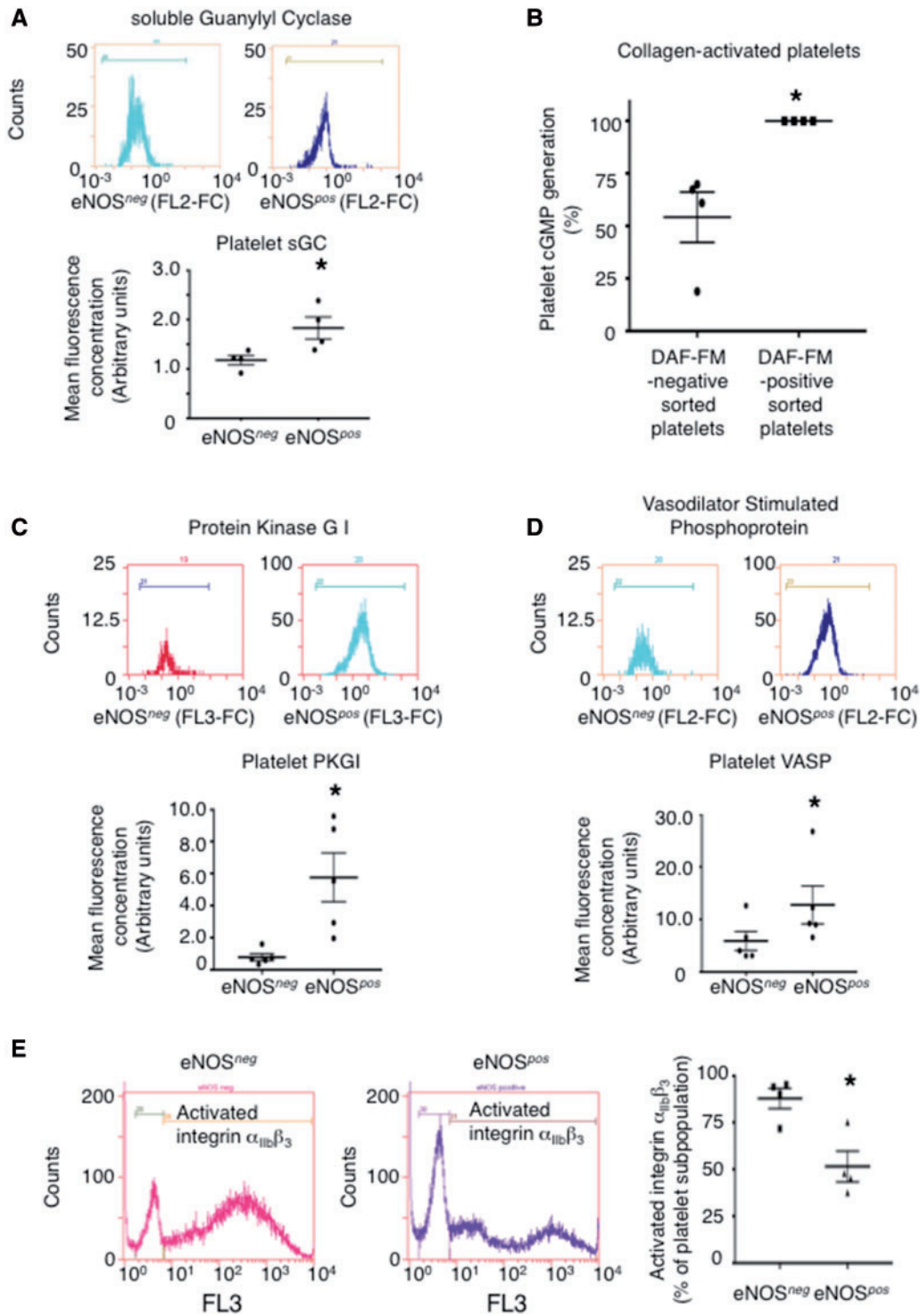


Figure 4 eNOS-negative platelets have a down-regulated sGC-PKG signalling pathway. (A) Summary data and representative histograms of sGC levels in eNOS-based platelet subpopulations, respectively. $N = 4$ independent experiments. $*P < 0.05$. (B) A comparison of cGMP generation by DAF-FM-negative vs. DAF-FM-positive FACS sorted platelets upon stimulation by collagen ($10 \mu\text{g}/\text{mL}$). $N = 4$. (C–D) Summary data and representative histograms of PKGI, and VASP levels in eNOS-based platelet subpopulations, respectively. $N = 5$. $*P < 0.05$. Antibody specificity for platelet sGC, PKGI, and VASP were confirmed in [Supplementary material online, Figure S14A–F](#). (E) Representative histograms along with summary data measuring activated $\alpha_{IIb}\beta_3$ (PAC-1 antibody) on eNOS^{neg} and eNOS^{pos} collagen-aggregated platelets. $N = 4$ independent experiments. $*P < 0.05$ vs. eNOS^{neg}.

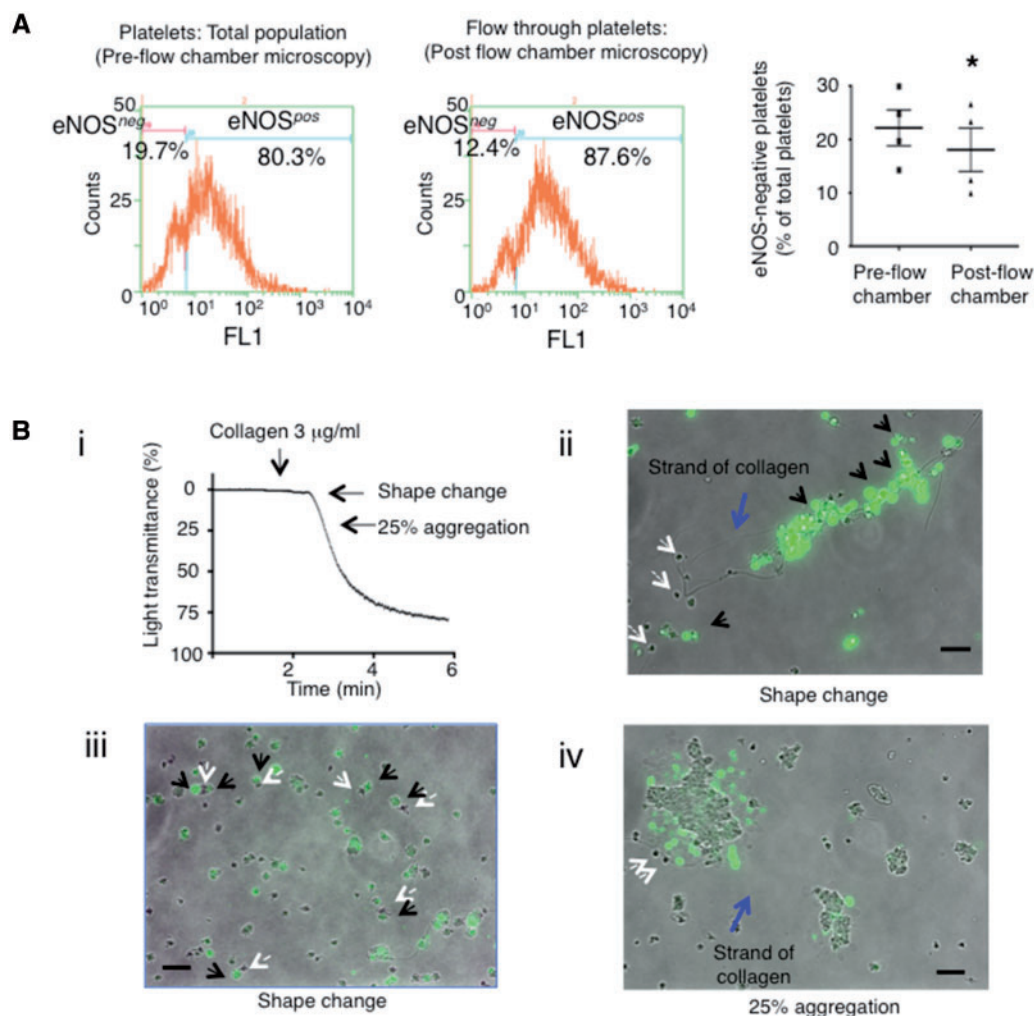


Figure 5 eNOS-negative platelets initiate adhesion and aggregation reactions. (A) Representative platelet eNOS^{neg} and eNOS^{pos} platelet flow cytometry histograms and summary data pre- and post flow chamber experiments. $N = 4$. $*P < 0.05$. (B) (i) Representative platelet aggregometry trace indicating time points at which DAF-FM-stained platelet samples were taken for fluorescence microscopy. (ii-iv) Merged brightfield-fluorescence microscopy images of non/low-NO-producing and NO-producing platelets binding to collagen strands (blue arrows) and each other (iii). Black arrows indicate platelets producing large amounts of NO. White arrows indicate platelets producing little/no NO. Images representative from $N = 3$ independent experiments. Bars indicate 10 μm .

recent years, others have questioned whether platelets contain NOS/eNOS.²⁶ However, these studies did not attempt to extract platelet membrane eNOS, which we demonstrate is likely localized in triton-resistant platelet caveolae, and used a relatively insensitive and indirect method of measuring NOS activity.³⁹ These authors speculated that detection of platelet NOS activity is due to contamination by iNOS-expressing leucocytes. Hence, we established sensitive and NO-specific flow cytometry and fluorescence microscopy protocols based on DAF-FM diacetate staining to detect platelet NO production. The use of DAF-based compounds as NO-specific indicators has been criticized recently⁴⁰; although, much of the criticism is based on studies that measured DAF fluorescence by tobacco plants treated with a fungal elicitor that generated a large amount of H(2)O(2) reaction products reacting with DAF-2⁴¹ and based on studies of 2, 3-diaminonaphthalene (DAN) that did not utilize DAF-FM.⁴² Nonetheless, to be certain of DAF-FM's specificity for platelet NO we performed pharmacological experiments

demonstrating that only L-NAME and AP-Cav-AB (classical NOS and eNOS-specific inhibitors) were able to reverse the increased fluorescence of DAF-FM-stained platelets activated in the presence of NOS substrate L-arginine.⁴³ Platelet-specific NO production was further confirmed with a second non-DAF-related fluorescent probe, a novel copper-based NO-indicator CuFLZE.⁴⁴ Using these methods we identified two platelet subpopulations, a larger NO-generating and a smaller non/low-NO-generating subpopulation. Consistent with earlier studies,^{12,13} platelets incubated with L-arginine that generated NO inhibited aggregation regardless of the platelet-activating stimulus concentration. This is important as it has been previously reported that L-arginine promotes the aggregation of platelets stimulated with a low concentration of thrombin, suggesting NO may have a biphasic effect; however, whether NO or ONOO⁻ was actually generated was not investigated.³¹ NO may react with O₂⁻ that may be generated when eNOS is uncoupled to form ONOO⁻, and ONOO⁻ has been demonstrated to potentiate

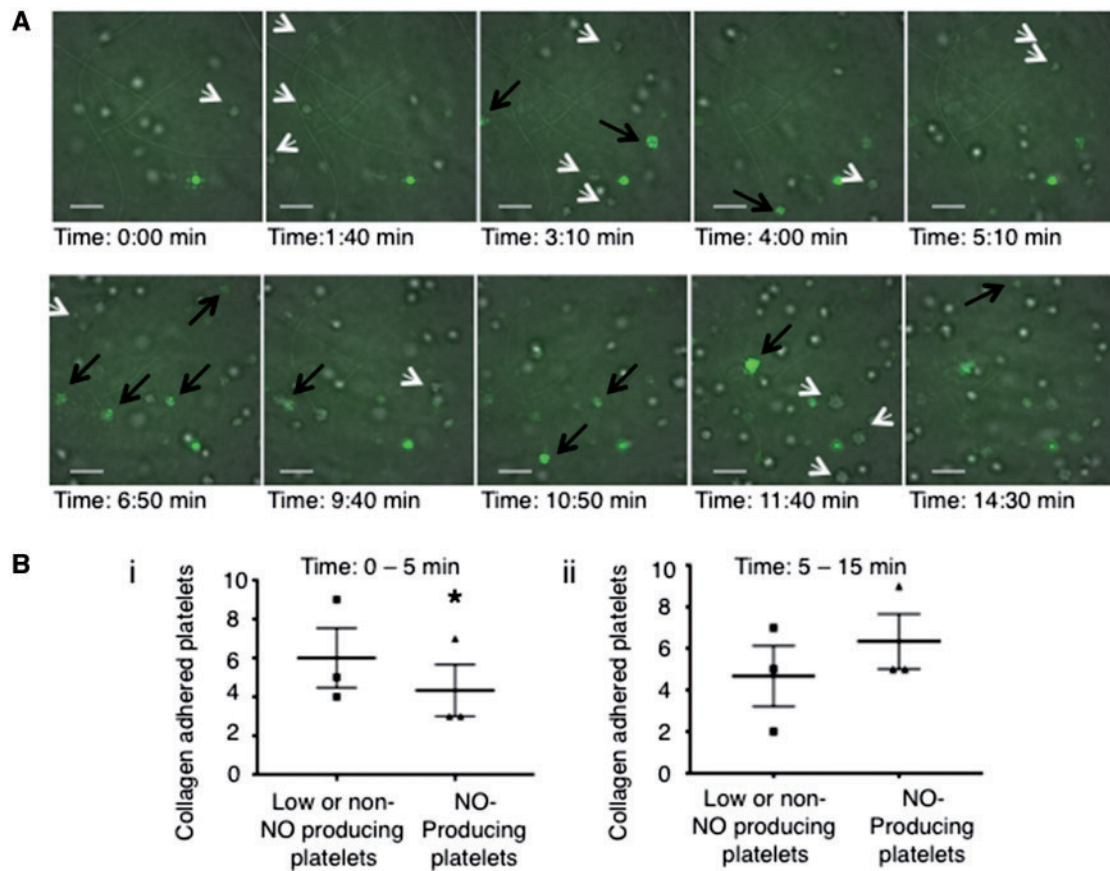


Figure 6 Confirmation that non-NO-producing platelets initiate adhesion and aggregation reactions while NO-producing platelets form the bulk of an aggregate and limit its size. (A) Merged brightfield-fluorescence microscopy frames from [Supplementary material online](#), video 1 of DAF-FM-loaded human platelets adhering to collagen-coated coverslips. White arrows indicate low/no-NO-producing platelets; black arrows indicate NO-producing platelets. Bars indicate 10 μm . (B) (i and ii) Summary data of low/non-NO-producing and NO-producing platelets binding to collagen over time from $N = 3$ independent experiments. $*P < 0.05$.

aggregation.³² Hence, we argue that NO, unless it reacts with O_2^- , only serves as a platelet negative-feedback regulator.

As NO could potentially diffuse from contaminating leucocytes and inhibit aggregation or react with platelet-trapped DAF-FM, we measured the leucocyte contamination in our platelet preparations. Flow cytometry measurements revealed leucocyte contamination of less than 0.002%. Previously, Vane and colleagues showed that leucocyte contamination of $>1\%$ can inhibit aggregation via a NO-dependent mechanism³⁰; therefore, the very few leucocytes in our platelet preparations cannot account for the inhibitory effects of platelet-generated NO in our experimental system. Moreover, the iNOS-selective antagonist 1400 W failed to reverse the inhibitory effects of L-arginine on aggregation further ruling out a possible involvement of iNOS-generated NO. Most importantly, video fluorescence microscopy of DAF-FM-loaded platelets demonstrated that adhering platelets generate NO independent of leucocytes. Consistent with our flow cytometry and fluorescence microscopy results, not all platelets generated NO upon adhesion to collagen in our videos. This finding is further consistent with a recent study by Cozzi and colleagues that utilized DAF-FM to visualize NO production by platelets during adhesion in flowing blood.⁴⁵ However, that study did not investigate or speculate on whether platelet subpopulations exist

with a differential ability to generate NO. Therefore, we investigated whether NO-producing and non-NO-producing platelets corresponded to platelet subpopulations with and without eNOS, respectively.

We developed a powerful flow cytometry protocol to measure intra-platelet eNOS, as immunoblotting is not sensitive enough to study eNOS-based platelet subpopulations following FACS-sorting (see [Supplementary material online](#), [Figure S19](#)). Using this protocol, we identified the presence of distinct eNOS^{neg} and eNOS^{pos} platelet subpopulations as measurements demonstrated bimodal histograms and not a Gaussian distribution of eNOS content. We named the platelets found within the lower histogram peak as eNOS^{neg} as this peak overlapped with isotype control antibody indicating an eNOS-negative subpopulation. Further, eNOS^{neg} and eNOS^{pos} platelets corresponded to non-NO-producing and NO-producing platelets as demonstrated by FACS sorting. Although FACS sorting was unable to purify the subpopulations to homogeneity, this was expected due to the small differences in DAF-FM fluorescence of NO-producing and non-NO-producing resting platelets and the high rate of sorting (15 000–20 000 events/s) necessary to collect enough platelets for further experiments. Importantly, eNOS^{neg} and eNOS^{pos} platelet subpopulations were also identified in eNOS-GFP transgenic mice, though unlike in humans the vast majority

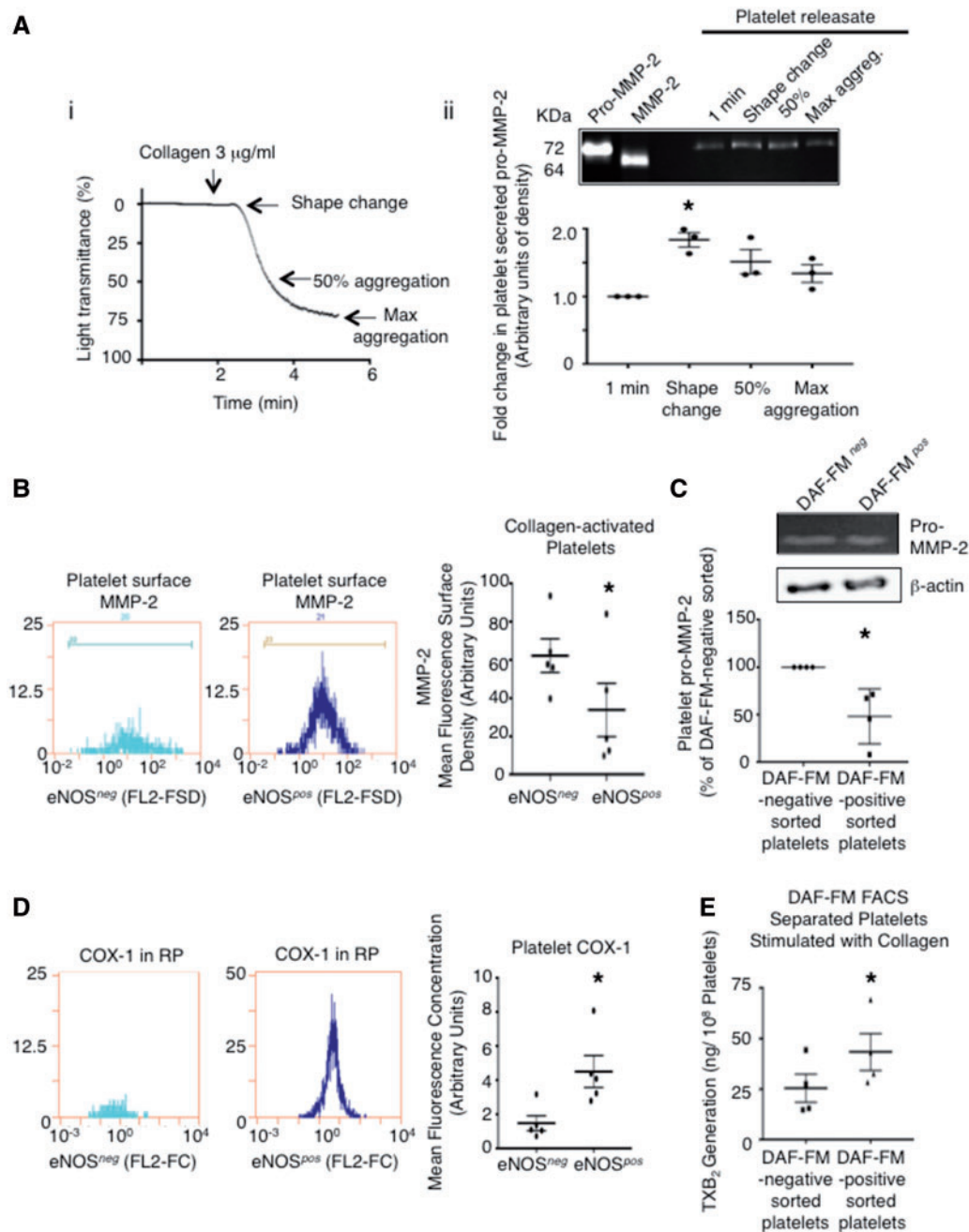


Figure 7 (A) (i) Representative platelet aggregometry trace indicating time points at which platelet releasates were taken for zymography analysis. (ii) Representative zymogram of the platelet MMP-2 secretion time course and summary densitometry data. $N = 3$ independent experiments. $*P < 0.05$. (B) Representative flow cytometer fluorescence surface density histograms and summary data of surface MMP-2 on collagen-activated (1 μg/mL) eNOS^{neg} and eNOS^{pos} platelets. $N = 5$. $*P < 0.05$. (C) Representative β-actin loading-controlled zymogram and summary data of platelet pro-MMP-2 within DAF-FM-negative and -positive FACS sorted platelet lysates. $N = 4$. $*P < 0.05$. (D) Representative intracellular flow cytometry fluorescence concentration histograms and summary data of COX-1 levels in eNOS^{neg} and eNOS^{pos} platelets. $N = 5$. $*P < 0.05$. (E) Summary LC-ESI-MS data of thromboxane generation by DAF-FM-negative and -positive FACS sorted platelets in response to collagen (10 μg/mL). $N = 4$. $*P < 0.05$.

of mouse platelets are eNOS^{neg} signifying that perhaps major differences in platelet NO-signalling exist between the two species. This species difference may explain why Ozuyaman *et al.* found eNOS-deficiency to not affect mouse platelet aggregation or bleeding time,⁴⁶ although Freedman *et al.* found eNOS-deficient mice to have shorter bleeding times and

enhanced platelet recruitment.²⁵ These disparate findings may also be influenced by factors such as mouse age and/or strain of eNOS-deficient mice. Importantly, to date, eNOS has not been identified in mouse or human platelets by mass spectrometry (MS),^{47–50} although most platelet MS studies have utilized shotgun MS approaches and have not targeted

eNOS identification directly, thereby potentially missing this relatively low abundance but important protein.

4.2 Potential origin of eNOS-based platelet subpopulations

The equivalent volumes and activated caspase-3 levels of human eNOS^{neg} and eNOS^{pos} platelets indicate that these platelet subpopulations are of the same circulatory age. Older studies of platelet aging suggested that platelets become smaller and less dense as they age.¹ More recently, it has been established that platelet life span is determined by an internal apoptotic clock governed by the ratio of platelet Bcl-x_L to Bak.⁵ As Bcl-x_L degrades over time pro-apoptotic Bak is freed and platelet apoptosis is induced activating caspase-3. Irrespective of the platelet-aging model, our data implies that eNOS^{neg} platelets are not older platelets that may have lost eNOS with time. Rather it suggests that they are simultaneously generated, which raises the intriguing question whether eNOS^{neg} and eNOS^{pos} megakaryocyte subtypes exist (Figure S20) that give rise to their respective platelet subpopulations? Mechanistically, a number of anti- and pro-inflammatory cytokines are known to counter-regulate endothelial eNOS expression.^{51,52} Hence, these same cytokines may regulate formation of eNOS^{neg} and eNOS^{pos} megakaryocyte subpopulations.

4.3 A novel conceptual model of platelet regulation

The discovery of biochemically distinct eNOS^{neg} and eNOS^{pos} platelets with differential functions has potential important implications for our understanding of haemostasis and thrombosis (see Supplementary material online, Figure S21). Based on our data, we propose that in response to vascular injury, eNOS^{neg} platelets first adhere to exposed collagen and/or vWF. This initial response results from the absence of endogenous NO generation coupled with refractoriness to NO because of a down-regulated sGC-PKG-signalling pathway within eNOS^{neg} platelets, thereby facilitating $\alpha_{IIb}\beta_3$ activation,⁵³ which stabilizes initial rolling, adhesion, and eNOS^{pos} platelet recruitment to site of injury. Further, we propose that eNOS^{neg} platelets secrete MMP-2, which promotes recruitment of eNOS^{pos} platelets to the forming aggregate. Next, eNOS^{pos} platelets form the bulk of an aggregate/thrombus due to their higher COX-1 content and greater thromboxane generation, but ultimately limit aggregate/thrombus size via NO generation as both increasing the ratio of eNOS-negative to -positive platelets or pharmacological inhibition of eNOS results in enhanced platelet aggregation. In addition to differentially regulating platelet plug formation, the roles of these platelet subpopulations in coagulation will require investigation. Fluorescence microscopy of collagen-adhering DAF-FM loaded platelets revealed membrane blebs/balloons with DAF-FM trapped NO. Recently, it has been reported that platelets can maximize their surface area through the coordinated formation of membrane balloons that enhance procoagulant spreading and amplify localized thrombin generation.⁵⁴ As eNOS^{pos} platelets aggregate overtop eNOS^{neg} platelets, they may be also ideally situated to regulate fibrin formation strengthening the initial platelet plug via formation of these balloons.

4.4 Nomenclature and potential clinical significance

Although we designate these platelet subpopulations eNOS^{neg} and eNOS^{pos}, the possibility exists that eNOS levels within eNOS^{neg} platelets may be below detection limits and that these subpopulations may

represent distinct eNOS^{low} or eNOS^{high} platelets. Nonetheless, potential alterations in the ratios of these subpopulations may predispose individuals to thrombotic or haemorrhagic events. Previous studies have reported that platelets from acute coronary syndrome (ACS) patients have impaired NO production,⁵⁵ and that platelet NO production correlates negatively with increasing number of coronary artery disease risk factors.⁵⁶ Similarly, platelet refractoriness to the NO-donor sodium nitroprusside was found to be predictive of increased morbidity and mortality in patients with high-risk ACS.⁵⁷ These previous clinical studies describe platelet responses that would be characteristic of eNOS^{neg} platelets (absence of eNOS and downregulation of sGC). Hence, an elevated ratio of eNOS^{neg}/eNOS^{pos} platelets may contribute to ACS etiology and other adverse cardiovascular events such as ischaemic stroke. If so, this raises the prospect that the ratio of eNOS^{neg}/eNOS^{pos} platelets may serve as an effective prognostic biomarker of these adverse cardiovascular events. Finally, further characterization of eNOS^{neg} and eNOS^{pos} platelets may offer the opportunity for early targeting of occlusive thrombus formation, drug development and improved anti-thrombotic therapy.

Supplementary material

Supplementary material is available at *Cardiovascular Research* online.

Acknowledgements

We thank D. Befus for discussions and critical review of our manuscript. We also thank D. Kratochwil-Otto for technical assistance.

Conflict of interest: none declared.

Funding

This work was funded by grants from the Canadian Institutes of Health Research MOP-130289 and OCN-126571 (P.J.), MOP-110967 (I.R.W.), and MOP-115037 (J.M.S.); an Alberta Innovates Health Solutions Postdoctoral Fellowship (A.R.B.), Graduate Studentship (H.E.S., A.A.E.S.) and Scholar Awards (J.M.S. and I.R.W.); and a Mike Wolowyk Graduate Scholarship (G.L.).

References

- Rand ML, Greenberg JP, Packham MA, Mustard JF. Density subpopulations of rabbit platelets: size, protein, and sialic acid content, and specific radioactivity changes following labeling with 35S-sulfate in vivo. *Blood* 1981;**57**:741–746.
- Thompson CB, Eaton K, Princiotta SM, Rushin CA, Valeri CR. Size dependent platelet subpopulations: relationship of platelet volume to ultrastructure, enzymatic activity, and function. *Br J Haematol* 1982;**50**:509–519.
- Dale GL, Friese P, Batar P, Hamilton SF, Reed GL, Jackson KW, Clemetson KJ, Alberio L. Stimulated platelets use serotonin to enhance their retention of procoagulant proteins on the cell surface. *Nature* 2002;**415**:175–179.
- London FS, Marcinkiewicz M, Walsh PN. A Subpopulation of platelets responds to thrombin- or SFLLRN-stimulation with binding sites for factor IXa. *J Biol Chem* 2004;**279**:19854–19859.
- Mason KD, Carpinelli MR, Fletcher JJ, Collinge JE, Hilton AA, Ellis S, Kelly PN, Ekert PG, Metcalf D, Roberts AW, Huang DCS, Kile BT. Programmed anuclear cell death delimits platelet life span. *Cell* 2007;**128**:1173–1186.
- Sawicki G, Salas E, Murat J, Miszta-Lane H, Radomski MW. Release of gelatinase A during platelet activation mediates aggregation. *Nature* 1997;**386**:616–619.
- Isenberg JS, Romeo MJ, Yu C, Yu CK, Nghiem K, Monsale J, Rick ME, Wink DA, Frazier WA, Roberts DD. Thrombospondin-1 stimulates platelet aggregation by blocking the antithrombotic activity of nitric oxide/cGMP signaling. *Blood* 2008;**111**:613–623.
- Moncada S, Gryglewski R, Bunting S, Vane JR. An enzyme isolated from arteries transforms prostaglandin endoperoxides to an unstable substance that inhibits platelet aggregation. *Nature* 1976;**263**:663–665.

9. Radomski MW, Palmer RMJ, Moncada S. Endogenous nitric oxide inhibits human platelet adhesion to vascular endothelium. *Lancet* 1987;**330**:1057–1058.
10. Provost P, Merhi Y. Endogenous nitric oxide release modulates mural platelet thrombosis and neutrophil-endothelium interactions under low and high shear conditions. *Thromb Res* 1997;**85**:315–326.
11. Loscalzo J. Nitric oxide insufficiency, platelet activation, and arterial thrombosis. *Circ Res* 2001;**88**:756–762.
12. Radomski MW, Palmer RM, Moncada S. An L-arginine/nitric oxide pathway present in human platelets regulates aggregation. *Proc Natl Acad Sci USA* 1990;**87**:5193–5197.
13. Radomski MW, Palmer R, Moncada S. Characterization of the L-arginine: nitric oxide pathway in human platelets. *Br J Pharmacol* 1990;**101**:325–328.
14. Malinski T, Radomski MW, Taha Z, Moncada S. Direct electrochemical measurement of nitric oxide released from human platelets. *Biochem Biophys Res Commun* 1993;**194**:960–965.
15. Radomski MW, Palmer RMJ, Moncada S. The role of nitric oxide and cGMP in platelet adhesion to vascular endothelium. *Biochem Biophys Res Commun* 1987;**148**:1482–1489.
16. Radomski MW, Palmer RMJ, Moncada S. Comparative pharmacology of endothelium-derived relaxing factor, nitric oxide and prostacyclin in platelets. *Br J Pharmacol* 1987;**92**:181–187.
17. Freedman JE, Loscalzo J, Barnard MR, Alpert C, Keane JF, Michelson AD. Nitric oxide released from activated platelets inhibits platelet recruitment. *J Clin Invest* 1997;**100**:350–356.
18. Moro MA, Russel RJ, Celtek S, Lizasoain I, Su Y, Darley-Usmar VM, Radomski MW, Moncada S. cGMP mediates the vascular and platelet actions of nitric oxide: confirmation using an inhibitor of the soluble guanylyl cyclase. *Proc Natl Acad Sci USA* 1996;**93**:1480–1485.
19. Halbrugge M, Friedrich C, Eigenthaler M, Schanzenbacher P, Walter U. Stoichiometric and reversible phosphorylation of a 46-kDa protein in human platelets in response to cGMP- and cAMP-elevating vasodilators. *J Biol Chem* 1990;**265**:3088–3093.
20. Smolenski A, Bachmann C, Reinhard K, Honig-Liedl P, Jarchau T, Hoschuetzky H, Walter U. Analysis and Regulation of Vasodilator-stimulated phosphoprotein serine 239 phosphorylation in vitro and in intact cells using a phosphospecific monoclonal antibody. *J Biol Chem* 1998;**273**:20029–20035.
21. Jurasz P, Stewart MW, Radomski A, Khadour F, Duszyk M, Radomski MW. Role of von Willebrand factor in tumour cell-induced platelet aggregation: differential regulation by NO and prostacyclin. *Br J Pharmacol* 2001;**134**:1104–1112.
22. Horstrup K, Jablonka B, Honig-Liedl P, Just M, Kochsiek K, Walter U. Phosphorylation of focal adhesion vasodilator-stimulated phosphoprotein at Ser157 in intact human platelets correlates with fibrinogen receptor inhibition. *Eur J Biochem* 1994;**225**:21–27.
23. Antl M, von Bruhl M-L, Eiglsperger C, Werner M, Konrad I, Kocher T, Wilm M, Hofmann F, Massberg S, Schlossmann J. IRAG mediates NO/cGMP-dependent inhibition of platelet aggregation and thrombus formation. *Blood* 2007;**109**:552–559.
24. Wang G-R, Zhu Y, Halushka PV, Lincoln TM, Mendelsohn ME. Mechanism of platelet inhibition by nitric oxide: in vivo phosphorylation of thromboxane receptor by cyclic GMP-dependent protein kinase. *Proc Natl Acad Sci USA* 1998;**95**:4888–4893.
25. Freedman JE, Sauter R, Battinelli EM, Ault K, Knowles C, Huang PL, Loscalzo J. Deficient platelet-derived nitric oxide and enhanced hemostasis in mice lacking the NOSIII gene. *Circ Res* 1999;**84**:1416–1421.
26. Gambaryan S, Kobsar A, Hartmann S, Birschmann I, Kuhlencordt PJ, Mller-Esterl W, Lohmann SM, Walter U. NO-synthase-/NO-independent regulation of human and murine platelet soluble guanylyl cyclase activity. *J Thromb Haemost* 2008;**6**:1376–1384.
27. Radomski M, Moncada S. An improved method for washing of human platelets with prostacyclin. *Thromb Res* 1983;**30**:383–389.
28. Valdez LB, Boveris A. Nitric oxide and superoxide radical production by human mononuclear leukocytes. *Antioxid Redox Signal* 2001;**3**:505–513.
29. Wykretowicz AFA, Szczpanik A, Wysocki H. Dipyrindamole inhibits hydroxylamine augmented nitric oxide (NO) production by activated polymorphonuclear neutrophils through an adenosine-independent mechanism. *Physiol Res* 2004;**53**:645–652.
30. Salvemini D, de Nucci G, Gryglewski RJ, Vane JR. Human neutrophils and mononuclear cells inhibit platelet aggregation by releasing a nitric oxide-like factor. *Proc Natl Acad Sci USA* 1989;**86**:6328–6332.
31. Marjanovic JA, Li Z, Stojanovic A, Du X. Stimulatory roles of nitric-oxide synthase 3 and guanylyl cyclase in platelet activation. *J Biol Chem* 2005;**280**:37430–37438.
32. Moro MA, Darley-Usmar VM, Goodwin DA, Read NG, Zamora-Pino R, Feelisch M, Radomski MW, Moncada S. Paradoxical fate and biological action of peroxynitrite on human platelets. *Proc Natl Acad Sci USA* 1994;**91**:6702–6706.
33. Bernatchez PN, Bauer PM, Yu J, Prendergast JS, He P, Sessa WC. Dissecting the molecular control of endothelial NO synthase by caveolin-1 using cell-permeable peptides. *Proc Natl Acad Sci USA* 2005;**102**:761–766.
34. Garcia-Cardena G, Oh P, Liu J, Schnitzer JE, Sessa WC. Targeting of nitric oxide synthase to endothelial cell caveolae via palmitoylation: implications for nitric oxide signaling. *Proc Natl Acad Sci USA* 1996;**93**:6448–6453.
35. van Haperen R, Cheng C, Mees BME, van Deel E, de Waard M, van Damme LCA, van Gent T, van Aken T, Krams R, Duncker DJ, de Crom R. Functional expression of endothelial nitric oxide synthase fused to green fluorescent protein in transgenic mice. *Am J Pathol* 2003;**163**:1677–1686.
36. Meyers KM, Seachord CL, Holmsen H, Smith JB, Prieur DJ. A dominant role of thromboxane formation in secondary aggregation of platelets. *Nature* 1979;**282**:331–333.
37. Sawicki GSE, Salas E, Wozniak M, Rodrigo J, Radomski MW. Localization and translocation of MMP-2 during aggregation of human platelets. *Thromb Haemost* 1998;**80**:836–839.
38. Jurasz P, Santos-Martinez MJ, Radomska A, Radomski MW. Generation of platelet angiotensin mediated by urokinase plasminogen activator: effects on angiogenesis. *J Thromb Haemost* 2006;**4**:1095–1106.
39. Böhmer A, Gambaryan S, Tsikas D. Human blood platelets lack nitric oxide synthase activity. *Platelets* 2015;**0**:1–6.
40. Gambaryan S, Tsikas D. A review and discussion of platelet nitric oxide and nitric oxide synthase: do blood platelets produce nitric oxide from L-arginine or nitrite? *Amino Acids* 2015;**47**:1779–1793.
41. Rümer S, Kirschke M, Fekete A, Mueller MJ, Kaiser WM. DAF-fluorescence without NO: elicitor treated tobacco cells produce fluorescing DAF-derivatives not related to DAF-2 triazol. *Nitric Oxide* 2012;**27**:123–135.
42. Tsikas D, Sandmann J, Beckmann B. Analysis of NO and its metabolites by mass spectrometry. Comment on 'Detection of nitric oxide in tissue samples by ESI-MS' by Z. Shen, A. Webster, K. J. Welham, C. E. Dyer, J. Greenman and S. J. Haswell. *Analyst* 2011;**136**:407–410.
43. Bode-Böger SM, Böger RH, Creutzig A, Tsikas D, Gutzki F-M, Alexander K, Frölich JC. L-Arginine infusion decreases peripheral arterial resistance and inhibits platelet aggregation in healthy subjects. *Clin Sci* 1994;**87**:303–310.
44. McQuade LE, Lippard SJ. Fluorescence-based nitric oxide sensing by Cu(II) complexes that can be trapped in living cells. *Inorg Chem* 2010;**49**:7464–7471.
45. Cozzi MR, Guglielmini G, Battiston M, Momi S, Lombardi E, Miller EC, De Zanet D, Mazzucato M, Gresele P, De Marco L. Visualization of nitric oxide production by individual platelets during adhesion in flowing blood. *Blood* 2015;**125**:697–705.
46. Ozyuyan B, Godecke A, Kusters S, Kirchhoff E, Scharf RE, Schrader J. Endothelial nitric oxide synthase plays a minor role in inhibition of arterial thrombus formation. *Thromb Haemost* 2005;**93**:1161–1167.
47. Zeiler M, Moser M, Mann M. Copy number analysis of the murine platelet proteome spanning the complete abundance range. *Mol Cell Proteomics* 2014;**13**:3435–3445.
48. Senis YA, Tomlinson MG, García Á, Dumon S, Heath VL, Herbert J, Cobbold SP, Spalton JC, Ayman S, Antrobus R, Zitzmann N, Bicknell R, Frampton J, Authi KS, Martin A, Wakelam MJO, Watson SP. A comprehensive proteomics and genomics analysis reveals novel transmembrane proteins in human platelets and mouse megakaryocytes including G6b-B, a novel immunoreceptor tyrosine-based inhibitory motif protein. *Mol Cell Proteomics* 2007;**6**:548–564.
49. Lewandrowski U, Wortelkamp S, Lohrig K, Zahedi RP, Wolters DA, Walter U, Sickmann A. Platelet membrane proteomics: a novel repository for functional research. *Blood* 2009;**114**:e10–e19.
50. Burkhardt JM, Vaudel M, Gambaryan S, Radau S, Walter U, Martens L, Geiger J, Sickmann A, Zahedi RP. The first comprehensive and quantitative analysis of human platelet protein composition allows the comparative analysis of structural and functional pathways. *Blood* 2012;**120**:e73–e82.
51. Cattaruzza M, Stodowski W, Stojakovic M, Krzesz R, Hecker M. Interleukin-10 induction of nitric-oxide synthase expression attenuates CD40-mediated interleukin-12 synthesis in human endothelial cells. *J Biol Chem* 2003;**278**:37874–37880.
52. Koh KP, Wang Y, Yi T, Shiao SL, Lorber MI, Sessa WC, Tellides G, Pober JS. T cell-mediated vascular dysfunction of human allografts results from IFN-g dysregulation of NO synthase. *J Clin Invest* 2004;**114**:846–856.
53. Roberts W, Michno A, Aburima A, Naseem KM. Nitric oxide inhibits von Willebrand factor-mediated platelet adhesion and spreading through regulation of integrin α IIb β 3 and myosin light chain. *J Thromb Haemost* 2009;**7**:2106–2115.
54. Agbani EO, van den Bosch MTJ, Brown E, Williams CM, Mattheij NJA, Cosemans JMEM, Collins PW, Heemskerk JWM, Hers I, Poole AW. Coordinated membrane ballooning and procoagulant-spreading in human platelets. *Circulation* 2015;**132**:1414–1424.
55. Freedman JE, Ting B, Hankin B, Loscalzo J, Keane JF Jr, Vita JA. Impaired platelet production of nitric oxide predicts presence of acute coronary syndromes. *Circulation* 1998;**98**:1481–1486.
56. Ikeda H, Takajo Y, Murohara T, Ichiki K, Adachi H, Haramaki N, Katoh A, Imaizumi T. Platelet-derived nitric oxide and coronary risk factors. *Hypertension* 2000;**35**:904–907.
57. Willoughby SR, Stewart S, Holmes AS, Chirkov YY, Horowitz JD. Platelet nitric oxide responsiveness: a novel prognostic marker in acute coronary syndromes. *Arterioscler Thromb Vasc Biol* 2005;**25**:2661–2666.